Pre-proofs version of the article "Electrochemical prevention of needle-tract seeding" (DOI: 10.1007/s10439-011-0295-4) to be published in Annals of Biomedical Engineering.

Title: Electrochemical prevention of needle-tract seeding

Antoni Ivorra *,[1]

[1] Dept. of Information and Communication Technologies, Universitat Pompeu Fabra, Barcelona, Spain

* Correspondig author

E-mail address: antoni.ivorra@gmail.com

Abstract:

Needle-tract seeding refers to the implantation of tumor cells by contamination when instruments, such as biopsy needles, are employed to examine, excise or ablate a tumor. The incidence of this iatrogenic phenomenon is low but it entails serious consequences. Here, as a new method for preventing neoplasm seeding, it is proposed to cause electrochemical reactions at the instrument surface so that a toxic microenvironment is formed. In particular, the instrument shaft would act as the cathode and the tissues would act as the electrolyte in an electrolysis cell. By employing numerical models and experimental observations reported by researchers on Electrochemical Treatment of tumors, it is numerically showed that a sufficiently toxic environment of supraphysiological pH can be created in a few seconds without excessive heating. Then, by employing an *ex vivo* model consisting of meat pieces, validity of the conclusions provided by the numerical model concerning pH evolution is confirmed. Furthermore, a simplified *in vitro* model based on bacteria, instead of tumor cells, is implemented for showing the plausibility of the method. Depending on the geometry of the instrument, suitable current densities will probably range from about 5 mA/cm^2 to 200 mA/cm^2 and the duration of DC current delivery will range from a few seconds to a few minutes.

Key terms: neoplasm seeding, needle-tract seeding, tumor cell dissemination, electrochemical treatment

Introduction

Neoplasm seeding refers to the local implantation of tumor cells by contamination of instruments and surgical equipment during and after surgical resection, resulting in local growth of the cells and tumor formation (definition according to the National Library of Medicine of the National Institutes of Health, USA). This iatrogenic artifact may occur, for instance, during laparoscopic interventions [1]. In the particular case of needle-shaped instruments, the term *needle-tract seeding* is employed to refer to the implantation of cells along the insertion path of the instrument. Examples of needle-shaped instruments in which neoplasm seeding has been reported are biopsy needles and radiofrequency ablation devices. Occurrence rates and clinical relevance of needle-tract seeding are a matter of debate. For breast cancer biopsies, incidence rates of clinical relevance diverge very significantly between studies, although it is admitted that it should be considered a matter of real concern [9]. In the case of biopsies of liver lesions, two recent reviews indicate that the risk of seeding is above 2 % [18, 19]. While the last figure may appear acceptably low, it has been recognized that chances of cure have been lost in some patients due to this phenomenon [11] and, consequently, it has been suggested to limit the indications for which percutaneous biopsy should be performed in the liver [20].

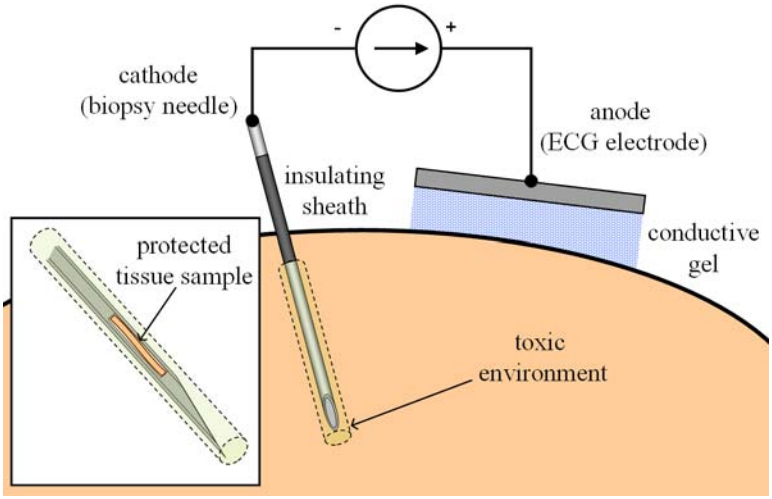

Figure 1. Illustration displaying the main elements of the proposed method for avoiding needle-tract seeding. A DC current is forced to flow through the biopsy needle (acting as cathode) so that a toxic microenvironment of high pH is created around the needle. Harvested samples in core biopsy needles will not be damaged since no electrochemical reactions will occur at the inner surfaces of the sample compartment. Some protective measures for minimizing undesired damage to healthy tissue are also depicted (see the text in the introduction section).

In order to prevent needle-tract seeding when percutaneous biopsies are harvested, at least two sorts of solutions have been reported: 1) biopsy devices including some sort of flexible sheath that avoids tumor cells from being dragged out through the insertion path [23] and 2) high temperature methods for causing cauterization or thermal ablation of adjacent tissues, either by heating the needle (US Patent App. 11/095,156, 2005) or by directly heating tissues around the needle by means of the Joule effect with radiofrequency currents [3, 10]. The first strategy has at least two obvious important drawbacks: it implies a significant modification of current biopsy devices that may result in thicker designs and, secondly, it does not minimize the chances of tumor spreading through bleeding or migration mechanisms. The heating strategy also presents some drawbacks. For instance, with thermal methods it will be necessary to control the actual temperature at the needle and its

surroundings, which implies at least a sensor at the probe tip, thus modifying current biopsy needle designs. Otherwise, excessive temperatures may cause the needle to stick to the tissues or, on the other hand, tissues may not be treated sufficiently [10]. More importantly, if precautions are not taken, heating may damage harvested biopsies. This is particularly important for most common designs of core biopsy needles in which the tissue sample, once excised, remains enclosed in a compartment very close to the needle tip and, therefore, would be exposed to heating as stainless steel is a very good heat conductor.

Here it is proposed a new method that may overcome the drawbacks of the previous ones: to provoke electrochemical reactions at the interface between the needle and the living tissues so that a toxic microenvironment is created around the needle. Such toxic microenvironment will not only kill tumor cells adhered to the needle but it will also minimize the chances of post-treatment neoplasm implantation by convection or migration as the needle-tract environment will remain toxic for some minutes. A very significant advantage of the proposed method is that, for a lot of current instruments, it will not imply any modification of their design.

Electrochemical reactions are those chemical reactions that occur at the interface between an electronic conductor (known as electrode) and an ionic conductor (known as electrolyte) which involve the transference of electrons between the electrode and the electrolyte species; when DC currents are allowed to flow through the interface between the electrode (e.g. a metal) and the electrolyte (e.g. biological media), oxidation and reduction chemical reactions occur which involve chemical species of the electrode and of the ionic medium. Some of the resulting chemical species liberated into the medium can damage tissue constituents or interfere with biological processes up to the point of compromising cell viability. At present, electrochemical reactions are intentionally induced with low level currents applied through metallic needles for the destruction of solid tumors in a procedure called *Electrochemical Treatment* (EChT) [14]. Typically, current densities in the order of 100 mA/cm^2 are applied for tens of minutes, or even hours, in order to create ablation zones with diameters in the order of some millimeters or a very few centimeters. Other employed names for the same technique are *Direct Current Treatment*, *Electrolytic Ablation* [6] and *Electrolysis* [4], however, this last term is more frequently used in the field of epilation, in which electrochemical reactions are caused in the vicinity of hair follicles for permanent hair removal [16].

In EChT, the main reactions that are believed to occur in biological samples when employing inert electrodes (e.g. platinum) are [14, 17], at the anode (i.e. the electrode connected to the positive pole of the generator):

$$2H_2O \Leftrightarrow O_2 + 4H^+ + 4e^- \qquad (1)$$

$$2Cl^- \Leftrightarrow Cl_2 + 2e^- \qquad (2)$$

and, at the cathode (i.e. the negative electrode):

$$2H_2O + 2e^- \Leftrightarrow H_2 + 2OH^- \qquad (3)$$

That is, at the anode the main reactions are the decomposition of water, which results in oxygen gas and a decrease of pH, and the oxidation of chloride ion, which results in chlorine gas. At the cathode the main reaction is the decomposition of water into molecular hydrogen (gas) and hydroxyl ions, which results in an increase of pH.

If, instead of inert electrodes such as platinum needles, electrochemically soluble electrodes are employed (e.g. copper, aluminum or stainless steel), then other oxidation reactions that release metallic ions can also occur at the anode [8], such as [17]:

$$2\,\mathrm{Al} \Leftrightarrow 2\,\mathrm{Al}^{+3} + 6\,\mathrm{e}^{-} \qquad (4)$$

The biological impact of each one of the above reactions and their resulting species is still a matter of debate. Nevertheless, it is mostly agreed that the induced pH alterations at the anode and the cathode are key factors determining the ablation capabilities of EChT [14]. As a matter of fact, it has been found that the spatial extent of pH alterations after current delivery is highly correlated with the extent of the injuries [4, 22].

In the context of the application discussed here, since most surgical instruments are made of stainless steel, which is an electrochemically soluble material, it appears more reasonable to make the instrument act as the cathode rather than as the anode. In principle, according to reaction 3, the cathode material will not be chemically damaged by the EChT treatment. Although it has been suggested that hydrogen bubbles cavitation may mechanically damage living tissues and the cathode surface [21], such kind of electrode damage was not noticeable in the experiments performed here (naked eye observations).

An illustration on how the proposed method would be implemented is displayed in figure 1: A current generator is connected to the instrument metallic shaft, which acts as cathode, and to a superficial electrode, which acts as anode and is also referred to here as *counter electrode*. Then, as time elapses, a toxic microenvironment of high pH develops around the cathode.

Since toxic species are not only created at the *working electrode* (i.e. the cathode) but also at the counter electrode, it is necessary to adopt some measures to prevent damage to the healthy tissues (i.e. skin) in contact with the counter electrode. A possible solution consists in placing an ionic conductor between the counter electrode and the skin, for instance, by means of an agar bridge (i.e. a solid gel containing free ions) or by means of conductive gels as those employed in electrophysiology. In this way, electrical conduction will still be possible but the electrochemically generated toxic species at the electrode interface will not have enough time to reach the skin.

The insulating sheath displayed in figure 1 is an optional feature intended to protect the skin. Prior to current delivery, it would be pushed some millimeters into the skin so that, locally, the electrochemical reactions would not occur on the interface between the instrument and the tissue therefore minimizing damage to the skin.

Since electrical currents are forced to flow through a resistive material (i.e. the tissue) some degree of Joule effect heating is unavoidable. Provided that the temperature does not reach the point of causing irreversible thermal damage (e.g. 55ºC for less than 10 seconds, [12]), which may accompanied by excessive protein denaturation and stickiness of tissues to the needle, such warming may be beneficial for the goal considered here as it will increase the toxicity of the method.

Once the main ideas of the proposed method have been exposed, a question that needs to be posed is the following: is it possible to create a toxic environment of sufficient toxicity and size around the instrument shaft in a short time so that the method can be clinically practical? Moreover, is it possible to do so without implying excessive Joule heating? Answering these questions is the goal of the study presented here. First, by taking into account some experimental observations from the EChT field and by employing numerical models also inherited form EChT researchers, it is numerically showed that a

sufficiently toxic environment can be created in a few seconds; such toxic environment would correspond to areas with excessive pH around the cathode. Then, by employing a simple *ex vivo* model, the validity of the conclusions provided by the numerical model concerning pH evolution are confirmed. Finally, for showing the plausibility of the method, an *in vitro* model was implemented in which the role of the tumor cells was played by innocuous bacteria contained in yogurt and the role of healthy tissue under risk was represented by an agar preparation suitable for lactobacillus colonization. Obviously, the numerical conclusions from that model should not be extrapolated to the clinical case as tumor cells and their environment are significantly different from the model conditions.

2. Methods

2.1. Numerical modeling

2.1.1 Equations of the pH model

The numerical model employed here was extracted from the model developed by Nilsson et al. for computing pH evolution around the cathode during electrochemical treatment of tissues [13]. In particular, the following significant simplifications were performed: water protolysis reversibility was disregarded, sodium and chloride ions migrations due to the electric field were also disregarded and the bicarbonate pH buffering system was not modeled as it was shown in their paper that bicarbonate buffering was very mild in comparison to organic constituents buffering. Another noteworthy difference with Nilsson's model is that here a cylindrical cathode is modeled instead of a spherical cathode.

Figure 2 shows the geometry of the model. The inner boundary represents the cathode/electrolyte interface where hydroxyl ions are created by electrolysis. Electrons required for the electrolysis flow into the electrolyte (i.e the tissue) through this inner boundary and are drawn by the outer boundary so that an electrical current flows through the electrolyte. The generated hydroxyl ions diffuse into the electrolyte and produce a local increase of pH. A portion of these hydroxyl ions are consumed in reactions with organic constituents of the tissue so that the pH increase is hampered (pH buffering). The equations that describe the model are presented below.

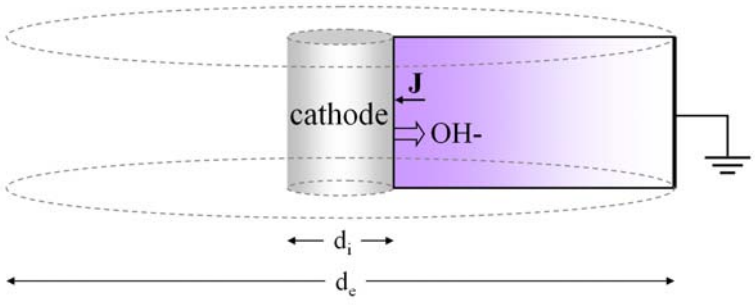

Figure 2. Geometry of the cylindrical model employed for the analysis. A flux of hydroxyl ions (OH-) is generated at the cathode/tissue interface (left boundary) by electrolysis due to an electrical current density (**J**). Then, such flux diffuses into the tissue and is partially consumed in irreversible reactions with the organic constituents of the tissue (i.e. buffering).

At the cathode surface the electrochemical production of hydroxyl ions is modeled as an inward flux according to Faraday's law under the assumption that the only electrochemical reaction that can occur at the cathode is the decomposition of water (i.e. upper estimate for hydroxyl ions production):

$$N_{\mathrm{OH-}} = \frac{|\mathbf{J}|}{F} \qquad (6)$$

Where $|\mathbf{J}|$ is the current density magnitude and F is the Faraday constant.

Then those ions are diffused into the electrolyte domain according to Fick's second law of diffusion:

$$\frac{\partial C_{\mathrm{OH-}}}{\partial t} = D_{\mathrm{OH-}} \nabla^2 C_{\mathrm{OH-}} \qquad (7)$$

Where $C_{\mathrm{OH-}}$ represents the concentration of hydroxyl ions, at each point of the electrolyte domain, and $D_{\mathrm{OH-}}$ is the diffusion constant for these ions.

A portion of the excess of hydroxyl ions created at the cathode surface irreversibly reacts with organic constituents (H_Org) of the tissues so that a pH buffering effect is produced:

$$\mathrm{H\_Org} + \mathrm{OH^-} \Rightarrow \mathrm{Org^-} + \mathrm{H_2O} \qquad (8)$$

The evolution of H_Org and OH^- concentrations ($C_{\mathrm{H\_Org}}$, $C_{\mathrm{OH-}}$) due to this reaction are modeled with the following reaction expressions:

$$R_{\mathrm{OH-}} = -k_{\mathrm{f}}\, C_{\mathrm{H\_Org}} C_{\mathrm{OH-}} + k_{\mathrm{f}}\, C^0_{\mathrm{H\_Org}} C^0_{\mathrm{OH-}} \qquad (9)$$

$$R_{\mathrm{H\_Org}} = -k_{\mathrm{f}}\, C_{\mathrm{H\_Org}} C_{\mathrm{OH-}} + k_{\mathrm{f}}\, C^0_{\mathrm{H\_Org}} C^0_{\mathrm{OH-}} \qquad (10)$$

Where $R_{\mathrm{OH-}}$ and $R_{\mathrm{H\_Org}}$ are the reaction rates (i.e. molar concentration per second) and k_{f} is the reaction constant that defines how fast these reactions happen as functions of the concentrations of hydroxyl ions and organic constituents.

The above reaction expressions 9 and 10 ensure that the buffering effect commences as soon $C_{\mathrm{OH-}}$ exceeds its initial concentration, $C^0_{\mathrm{OH-}}$, which is the concentration of hydroxyl ions in water before electrolysis begins.

Since the concentration of OH^- in the electrolyte domain not only depends on the diffusion of OH^- created at the cathode interface but also on the buffering reactions, a new term is included to equation 6 for defining the evolution of $C_{\mathrm{OH-}}$:

$$\frac{\partial C_{\mathrm{OH-}}}{\partial t} = D_{\mathrm{OH-}} \nabla^2 C_{\mathrm{OH-}} + R_{\mathrm{OH-}} \qquad (11)$$

Similarly, the evolution of $C_{\mathrm{H\_Org}}$ is modeled as:

$$\frac{\partial C_{\mathrm{H\_Org}}}{\partial t} = R_{\mathrm{H\_Org}} \qquad (12)$$

Finally, the pH value is computed as:

$$\mathrm{pH} = \mathrm{p}K_W - \mathrm{pOH} = -\log_{10}(K_W) + \log_{10}(C_{\mathrm{OH-}}) \qquad (13)$$

Where K_W is the self-ionization constant of water at 37ºC ($10^{-13.6}$ M^2).

To sum up, the concentration evolution of two chemical species, OH^- and H_Org, is modeled in a homogenous and isotropic medium. OH^- ions are created at the cathode interface according to the Faraday's law and diffuse into the medium where some of them are consumed in irreversible reactions with static H_Org molecules.

2.1.2 Electro-Thermal equations

Current flowing through the electrolyte causes heat according to Joule's first law:

$$q = |\mathbf{J}|^2 \rho_e \qquad (14)$$

Where q is the amount of heat (watts) generated per unit of volume, $|\mathbf{J}|$ is the current density magnitude and ρ_e is the electrical resistivity of the electrolyte (inverse of the conductivity, σ_e).

Local heat generated by the Joule effect is dissipated in living tissues mostly by heat conduction and by blood perfusion. Here, in order to predict the maximum temperature that is reached due to the electrochemical treatment, the worst scenario is selected: the thermal effect of blood perfusion is considered as null. Therefore, the differential equation that models the temperature (T) evolution is:

$$\rho c \frac{\partial T}{\partial t} = k \nabla^2 T + q \qquad (15)$$

Where ρ is the mass density of the tissue, c the heat capacity and k is the thermal conductivity constant.

2.1.3 Numerical implementation and input data

The numerical solutions were computed on a commercial Finite Element Method software platform: COMSOL Multiphysics 3.5 (COMSOL AB, Stockholm, Sweden). Four interdependent 'application modes' with axial symmetry (2D) and employing the same geometry were created: a 'Convection and Diffusion' mode for the concentration of hydroxyl ions, another 'Convection and Diffusion' mode for the concentration of H_Org, a 'Conductive Media DC' mode for computing Joule heating due to the current density applied for electrolysis and, finally, a 'Heat Transfer by Conduction' mode for modeling the temperature increase due to the Joule heat. The finite element mesh was made of rectangular elements that had a height equal to the domain height, that is, the problem was defined as a 2D geometry but it was in fact solved as a 1D geometry (such absurdity was motivated by the lack of a 'Conductive Media DC' mode in the 1D axial symmetry set of COMSOL Multiphysics 3.5). The number of mesh elements was 500 with increasing wideness form the inner boundary to the outer boundary. Time transient analyses for up to 10 minutes after current pulse conclusion were performed. Different current densities and durations of the current pulses were tried. In particular, the three simulations reported here in section 3.1 correspond to a pulse of 500 mA/cm^2 and 5 seconds, a pulse of 200 mA/cm^2 and 5 seconds and a pulse of 6.4 mA/cm^2 and 60 seconds. The diameter of the cathode (d_i) in those simulations was 1 mm whereas the diameter of the domain (d_e) was 20 mm. For the simulation results reported in section 3.2 the cathode diameter was 0.7 mm. The rest of numerical values employed in the simulations are detailed in Table 1 and correspond to generic animal soft tissues.

Table 1. Physical and chemical input values to the model

Parameter	Value	Reference
D_{OH^-} ($cm^2\ s^{-1}$)	7.05×10^{-5}	[13]
k_f ($M^{-1}\ s^{-1}$)	1.5×10^{11}	[13]
$C^0_{OH^-}$ (M)	6.31×10^{-7}	[13]
$C^0_{H\_Org}$ (M)	0.05	[13]
K_W (M^2)	$1 \times 10^{-13.6}$	[13]
F ($C\ mol^{-1}$)	96485	-
σ_e ($S\ m^{-1}$)	0.1	[5]
ρ ($kg\ (m^3)^{-1}$)	1000	[2]
c ($J\ kg^{-1}\ K^{-1}$)	3750	[2]
k ($W\ m^{-1}\ K^{-1}$)	0.5	[2]
T_0 (K)	310	-

2.2. *Ex vivo* experiments

For validating the usefulness of the model employed above regarding pH evolution in the case of mild treatments (in comparison to whole tumor ablation in EChT), a small series of unsophisticated *ex vivo* experiments was carried out on pieces of pork loin acquired from a retailer. The pieces had a thickness of about 11 mm or 12 mm. Two hypodermic stainless steel needles with a diameter of approximately 0.7 mm (21 G) were inserted through the meat pieces in a parallel fashion at a separation distance of about 10 mm. One of the needles (the cathode) was connected to the negative pole of a custom built constant current generator and the other needle (the anode) was connected to the positive pole. Four DC current magnitudes were employed depending on each specific experiment: 10 mA, 25 mA, 100 mA and 200 mA, which yield current densities at the electrodes of approximately 40 mA/cm^2, 100 mA/cm^2, 400 mA/cm^2 and 800 mA/cm^2 respectively. After switching on the current supply, time was monitored with a chronometer, and current was switched off at 5, 10, 30 or 60 seconds depending on the specific experiment. In particular, the following combinations were tried: 10 mA for 60 s, 25 mA for 30 s, 25 mA for 60 s, 100 mA for 10 s, 100 mA for 30 s, 100 mA for 60 s, 200 mA for 5 s and 200 mA for 10 s. Additionally, two control experiments, consisting in applying 0 mA for 30 s, were also performed.

After switching off the current, the needles were removed and the pork piece was immediately cut in half (needles axes perpendicular to this cut). Then, a pH indicator strip (ref CZ-9013, Instruments Direct (Services) Ltd., Coalville, Leicestershire, UK) was placed and gently pressed on the spot were the needle acting as cathode was. After about two seconds the pH strip was examined and a picture of it was taken. Time elapsed between switching off current and pH strip placement on the affected area was about 10 seconds.

The pH strips employed here have an active area of 5 mm × 5 mm that turns from yellow to brown-violet at pH values equal or higher than 12. Interestingly, if sample is not too wet so that smearing is prevented, a nice ‘map’ of pH levels can be obtained.

2.3. Proof of concept with an *in vitro* bacterial model

As a proof of concept of the method proposed here, an *in vitro* model was implemented in which the role of the tumor cells was played by innocuous bacteria (Lactobacillus bulgaricus contained in commercial yogurt) and the role of healthy tissue under risk was represented by

an agar plate suitable for bacteria colonization. The model is schematically represented in Figure 3: a plastic Petri dish (diameter = 55 mm, height = 14 mm) containing the agar preparation suitable for lactobacillus growth (1.5 g of agar powder (catalogue code 401792 by Panreac Química, S.A.U., Castellar del Vallès, Spain) per 100 ml of distilled water + 5.5 g of MRS broth powder (catalogue code 38944 by Sigma-Aldrich, Co., St. Louis, MO, USA) per 100 ml of water) is placed downwards on another identical Petri dish containing commercial yogurt (Carrefour Discount brand). Holes are made on the bottom of the agar Petri dish so that stainless steel syringe needles (diameter ~ 0.7 mm, 21G) can be inserted through the agar and the yogurt. Then, the electrochemical treatment is applied between two needles: one of the needles, in the center of the Petri dish, acts as the anode (i.e. counter electrode) and the other one in the periphery acts as the cathode (i.e. working electrode). A few seconds after treatment conclusion (~ 5 seconds), the needle acting as the cathode is carefully pulled out. Then, another hole is made in another location of the periphery and the procedure is repeated (if the cathode needle is reused then it is sterilized with ethanol 70% and rinsed with deionized water before insertion). In most of the experimental cases reported here, four experiments were performed for each agar dish; two of those experiments were controls (no delivery of current) and in the other two experiments a constant level of current was delivered for a limited amount of time. The amount of current that was delivered was calculated for selected current densities (10 mA/cm^2, 20 mA/cm^2 or 100 mA/cm^2) after measuring the thickness of the agar preparation and the yogurt and under the assumption that the conductivity of the agar preparation was similar to that of yogurt (σ_{yogurt} = 0.6 S/m, $\sigma_{agar\ preparation}$ = 0.8 S/m; measured here with and LCR meter at 10 kHz, Agilent U1732A, in electroporation cuvettes, catalog number 165-2082 of Bio-Rad Laboratories, Inc.).

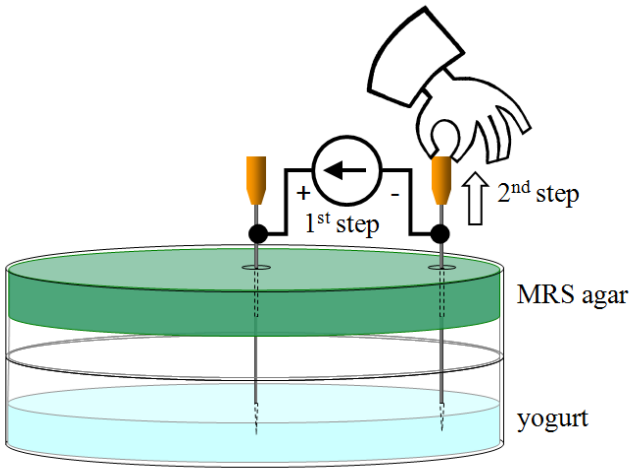

Figure 3. Schematic representation of the proof of concept experiments.

After conclusion of the treatments, the holes on the bottom of the agar Petri dishes were sealed with tape and the agar Petri dishes were kept in an oxygen depleted jar at 42 ºC for 24 hours as indicated in "Cultivation of bacteria from commercial yogurt" (http://www.umsl.edu/~microbes/pdf/cultivatingyogurt.pdf). Under these conditions (i.e. high temperature and low level of oxygen), bacteria grow to form visible colonies within the needle tracts that did not receive any treatment. At the end of the 24 hours incubation, each one of the needle tracts was carefully excised (cuboids of approximately 5 mm × 5 mm × 7 mm with the needle tract as the longest axis) and examined (naked eye and ×5 magnifying lens) for assessing whether or not bacteria colonies were present.

3. Results and discussion

3.1 Numerical modeling results

Cell death due to supraphysiological pH will depend both on the pH values that are reached and on the duration of the insult [22]. No experimental studies have been found in which the two parameters are independently analyzed. Yet in two studies on EChT it is reported that electrochemically ablated regions around the cathode correspond to areas with a pH over 9 [4, 22]. Since EChT procedures imply long exposure times of tens of minutes, it seems reasonable to assume that the areas in which a pH over 9 resulted in damage were exposed to such insult for some minutes. Then, as a criterion for forecasting treatment outcome, here it is considered that cells will be killed when exposed to pH $\geq$ 9 for over 5 minutes.

Figure 4.a shows the modeled evolution of pH after delivery of a DC current density of 500 mA/cm^2 for 5 seconds. As hydroxyl ions diffuse into the medium the pH front advances and reaches a distance of about 2 mm at 10 minutes. Naturally, at this late stage the concentration of hydroxyl ions is lower than the concentration immediately after current pulse conclusion as such maximum concentration dilutes by diffusion and it is also partially consumed by the buffering reactions with organic constituents. Nevertheless, after 10 minutes the pH is still well above 9 up to a distance of about 1.8 mm. Therefore, according to the criterion selected for cell damage forecasting, the thickness of the ablated region around the cathode will be between 1.5 and 2 mm. This outcome will not only be safe enough for seeding prediction but may be also considered as overtreatment.

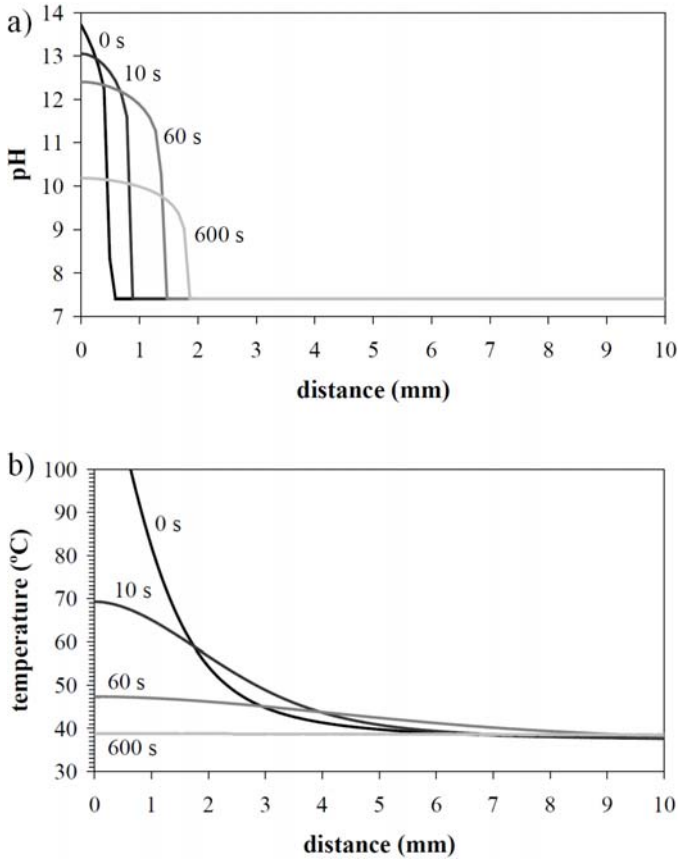

Figure 4. Numerically modeled pH and temperature evolution around a cylindrical cathode with a diameter of 1mm inserted in a saline solution with a conductivity of 0.1 S/m when a DC current of 500 mA/cm^2 is applied for 5 seconds. The labels on the plots indicate elapsed time after pulse conclusion.

For the same model, figure 4.b shows that the temperature around the cathode reaches values above the water boiling point, which obviously will be accompanied by thermal damage to the adjacent tissues and to the hypothetical sampled tissue. Although, in this case, excessive temperature increase will result in overtreatment (independent on the possible overtreatment caused by hydroxyl ions production), temperature increase cannot be considered as an adverse consequence in all cases provided that it does not reach the point of damaging the sample or causing excessive coagulation of adjacent tissues so that the needle cathode sticks to the tissues. In relation to the last cited outcome, needle stickiness, it must be noted that some of the conditions tried during the series of *ex vivo* experiments (section 3.2), which caused more heat than the protocol modeled here, did not produce observable desiccation or stickiness. Nevertheless for demonstrating that similar electrochemical outcomes can be obtained without excessive heat, the same model was computed with a current density of 200 mA/cm^2 instead of 500 mA/cm^2 (see Figure 5). In this case the pH values are lower than in the previous case but still the thickness of the ablated region is close to 1 mm (criterion of 5 minutes of pH above 9), which seems more than safe enough for preventing seeding. On the other hand, the maximum temperature is 52 ºC and, since it only lasts a few seconds, no heat damage can be expected.

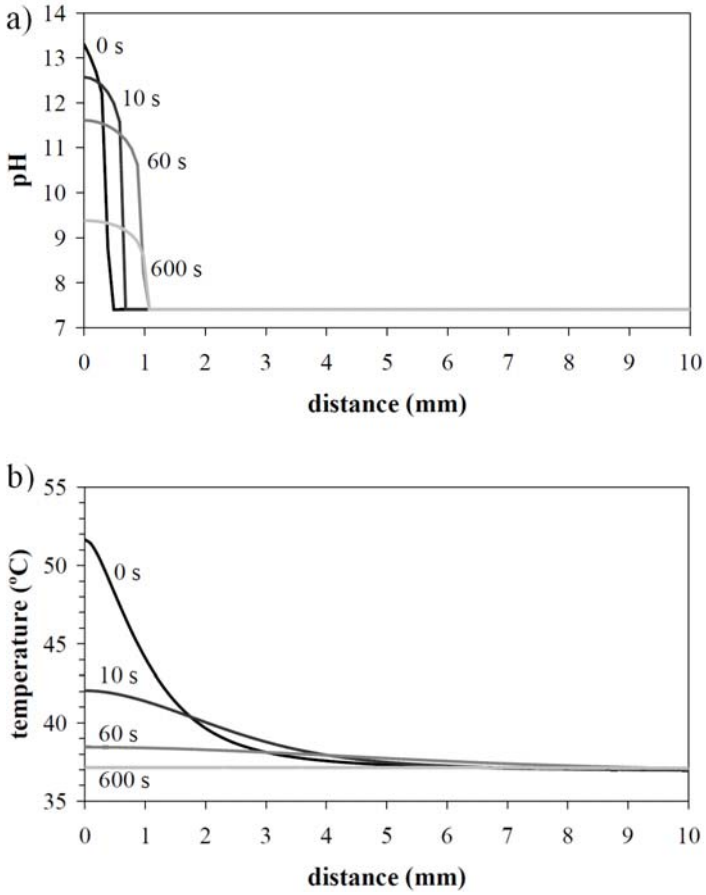

Figure 5. Same as figure 4 for a DC current of 200 mA/cm^2 applied for 5 seconds.

Therefore, according to the numerical model and the assumptions made here, in a few seconds it is possible to electrochemically create a toxic environment of sufficient toxicity

and size around an instrument shaft with a diameter in the order of 1 mm without generating excessive heat.

Nonetheless it must be noted that heating may not be the only restrictive factor that needs to be taken into account when selecting the magnitude and duration of the current pulse. Regarding heart arrhythmia induction, DC currents are considered much safer than AC currents with frequencies in the order of 50 Hz. However, DC currents can also cause muscle tetanus, which is obviously unpleasant, and can provoke heart arrhythmias if excessive. For instance, in the clinical use of EChT for lung cancer treatment it has been reported a case in which reversible "blockage of heart beat" occurred when the electrodes were located too close to the heart (<3 cm) and a current between 40 mA and 80 mA was delivered [24]. Therefore it seems sensible to restrict the maximum deliverable current depending on the area of treatment and other circumstances. It is out of the scope of the present study to set such current limits. As a first approach, a reasonable limit would be 20 mA since it appears to be the maximum level of current employed in electrolytic epilation [15]. For that current magnitude, in the hypothetical, but plausible, case of a 10 cm long shaft with a diameter of 1 mm, the maximum current density would be 6.4 mA/cm^2 if the instrument is completely inserted into the body. In this case, according to simulations (not reported here due to size constrains), a single pulse of 5 seconds would be unable to generate enough hydroxyl ions for damaging cells on the cathode surface; much longer pulses would be required. For instance, a pulse of 6.4 mA/cm^2 and 60 seconds would produce an ablated thickness in the order of 200 μm. On one hand, the use of very low current densities may be interesting as it limits damage to healthy tissues but, on the other hand, it makes the method more cumbersome, as it requires more time, and may compromise the safety of the method regarding seeding prevention. Therefore, in view of these results it is obvious that the current study must be followed by further *in vitro* and *in vivo* studies for assessing the feasibility of the proposed method.

3.2 *Ex vivo* experiments results

Figure 6 displays some pictures of the pH indicator strips applied to the meat pieces approximately 10 seconds after the electrochemical treatment. For each picture, the brown-violet area corresponds to the region around the cathode location with a pH equal or larger to 12. The smaller and larger diameters of these regions were measured and are presented in table 2 together with the values obtained from equivalent simulations. The correlation between the dimensions of the regions of pH ≥ 12 as observed on the pH indicator strips and the diameters of the regions of pH ≥ 12 as predicted by the simulations is convincingly good (the R^2 correlation value is 0.805 for the mean diameter). There appears to be a slight overestimation in the prediction, particularly for low dose conditions, but overall it can be stated the numerical model produces sufficiently accurate predictions, at least for the purposes of the current study.

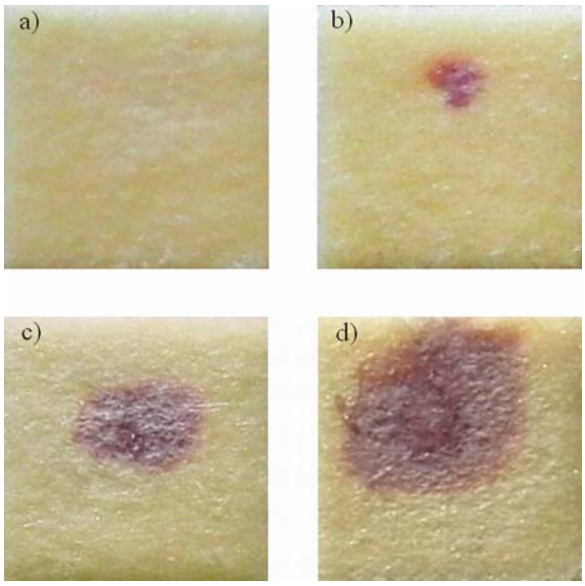

Figure 6. Pictures of the active area (5 mm × 5 mm) of the pH indicator strips (dark violet indicates pH ≥ 12) after pressing them against the meat region where the electrode was during the electrochemical treatment. a) 0 mA for 30 s, b) 100 mA/cm^2 for 60 s, c) 400 mA/cm^2 for 30 s and d) 400 mA/cm^2 for 60 s.

Table 2. Simulated and experimentally obtained regions with a pH over 12 for different current pulses.

Conditions |J| (mA/cm^2), duration (s)	Simulated $Ø_{(pH>12)}$ (mm)	Simulated $Ø_{(pH>12)}$ - 0.7 (mm)	Obtained $Ø_{(pH>12)}$ smallest, largest (mm)
0, 30	0	0	0
40, 60	2.3	1.6	0.9, 1.0
100, 30	2.3	1.6	0.6, 0.8
100, 60	3.0	2.3	1.1, 1.2
400, 10	2.3	1.6	1.1, 1.5
400, 30	3.2	2.5	2.0, 2.6
400, 60	4.1	3.4	3.5, 3.7
800, 5	2.2	1.5	1.0, 1.2
800, 10	2.6	1.9	1.7, 2.4

Note: Better correspondence is obtained when the diameter of the needle is subtracted from the simulation result; this would be explained by the fact that the tissue orifice collapses as the needle is pulled out. The experimentally obtained region of pH above 12 is approximated by an ellipse and the smallest and largest diameters of that ellipse are noted in the fourth column.

3.3. Proof of concept results

As indicated in section 2.3, after incubation, the needle tracts were carefully examined for assessing whether or not bacteria colonies were present. The picture displayed in Figure 7 shows two examples of obtained needle tracts. The clean needle tract on left corresponds to a case in which an efficient electrochemical treatment was applied whereas the dirty needle tract on the right corresponds to a control case (i.e. no electrochemical treatment).

All the protocols (current density and duration) assayed with this proof of concept model are presented in table 3. As expected, the resulting colonization rates indicate that minimum thresholds for current density and duration must be reached for achieving effective sterilization. It is interesting to note that the protocol consisting of a current density of 10 mA/cm^2 and 60 s, which is similar to protocol of uncertain efficiency simulated in figure 6, seems to be partially efficient. Nonetheless, despite this coincidence, no numerical conclusions should be extracted from these results regarding the efficacy of the protocols assayed here for the case of neoplasm seeding; several significant factors differ between the two scenarios (e.g. physiology of tumor cells versus the physiology of bacteria).

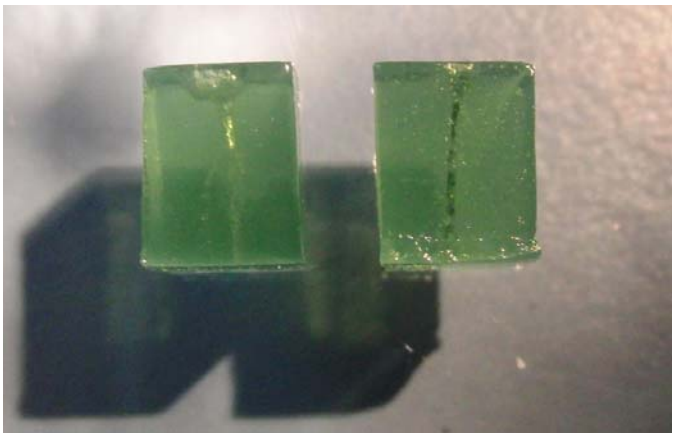

Figure 7. Picture of two needle tracts in MRS agar at 24 hours of incubation after treatment. The clean needle tract on left corresponds to a case in which an efficient electrochemical treatment was applied (100 mA/cm^2 for 30 s) whereas the dirty needle tract on the right (black spots are bacteria colonies) corresponds to a control case (0 mA/cm^2 for 30 s)

Table 3. Assayed protocols with the bacterial proof of concept model and related results.

Conditions		Bacterial colonization cases /
$\|\mathbf{J}\|$ (mA/cm^2)	duration (s)	total cases (rate %)
0	30	10/11 (91 %)
10	10	2/2 (100 %)
10	30	1/1 (100 %)
10	60	1/3 (33 %)
20	60	0/2 (0 %)
100	10	0/2 (0%)
100	30	0/5 (0 %)
100	60	0/2 (0 %)

Conclusion

Here, as a new method for preventing neoplasm seeding along needle tract, it has been proposed to provoke electrochemical cathodic reactions at the needle surface so that a toxic microenvironment is formed.

According to the numerical model and the assumptions made here, in a few seconds it will be possible to electrochemically generate a toxic environment of sufficient toxicity

and size around an instrument shaft with a diameter in the order of 1 mm without generating excessive heat. Such treatment will imply current densities in the order of 100 mA/cm^2. If, for any reason besides heating, the amount of deliverable current is limited and, consequently, the current density has to be decreased to magnitudes in the order of 10 mA/cm^2 then the treatment will have to be significantly longer (in the order of a single minute or a very few minutes). The validity of the numerical model employed for predicting pH values immediately after treatment has been reinforced by means of an *ex vivo* tissue model.

For showing the plausibility of the method, a crude *in vitro* model has been implemented in which the role of the tumor cells has been played by bacteria and the role of healthy tissue under risk has been played by a gelatinous preparation suitable for bacteria colonization. The electrochemical treatment indeed did prevent the colonization of bacteria within needle tracts left in the gelatinous preparation. Obviously, the numerical conclusions extracted from that model must not be extrapolated directly to the clinical case as tumor cells and their environment are significantly different from the model conditions.

The proposed electrochemical method can be accompanied, intentionally or unintentionally, by Joule thermal damage and by irreversible electroporation [7]. In particular, since electroporation can be accompanied by undesirable neuromuscular stimulation, Joule heating would be a convenient adjuvant method. As a matter of fact, such combination is already employed in epilation devices in which the DC current causing the electrochemical damage is superposed to an AC current causing diathermy.

The presented study will be followed by literature research, numerical studies and, probably, large animal experimentation for finding out maximum allowable DC currents in different clinical scenarios such as core breast biopsy. In addition, *in vivo* experimentation with aggressive tumors implanted in immunosuppressed rodents will be carried out for demonstrating the efficacy of the method for preventing needle-tract seeding.

Acknowledgements

Lluis Mir, director of the laboratory UMR 8203 of the Centre National de la Recherche Scientifique (Villejuif, France), provided comments and suggestions that helped to improve the quality of the manuscript.

AI's research is currently supported by a Ramón y Cajal fellowship from the Spanish Ministry for Science and Innovation.

References

1. Castillo, O. A. and G. Vitagliano. Port site metastasis and tumor seeding in oncologic laparoscopic urology. Urology 71:372-378, 2008.

2. Davalos, R. V., B. Rubinsky, and L. M. Mir. Theoretical analysis of the thermal effects during in vivo tissue electroporation. Bioelectrochemistry 61:99-107, 2003.

3. Dromi, S. A., J. Locklin, and B. J. Wood. Radiofrequency cauterization: an alternative to reduce post-biopsy hemorrhage. Cardiovasc. Intervent. Radiol. 28:681-682, 2005.

4. Finch, J. G., B. Fosh, A. Anthony, E. Slimani, M. Texler, D. P. Berry, A. R. Dennison, and G. J. Maddern. Liver electrolysis: pH can reliably monitor the extent of hepatic ablation in pigs. Clin. Sci. (Lond) 102:389-395, 2002.

5. Gabriel, C., S. Gabriel, and E. Corthout. The dielectric properties of biological tissues: I. Literature survey. Phys. Med. Biol. 41:2231-2249, 1996.

6. Gravante, G., S. L. Ong, M. S. Metcalfe, N. Bhardwaj, G. J. Maddern, D. M. Lloyd, and A. R. Dennison. Experimental application of electrolysis in the treatment of liver and pancreatic tumours: Principles, preclinical and clinical observations and future perspectives. Surg. Oncol. , 2009.

7. Ivorra, A. "Tissue Electroporation as a Bioelectric Phenomenon: Basic Concepts." In: Irreversible Electroporation, edited by B. Rubinsky. : Springer Berlin Heidelberg, 2010, pp. 23-61.

8. Kotnik, T., D. Miklavcic, and L. M. Mir. Cell membrane electropermeabilization by symmetrical bipolar rectangular pulses. Part II. Reduced electrolytic contamination. Bioelectrochemistry 54:91-95, 2001.

9. Kwo, S. and J. C. Grotting. Does stereotactic core needle biopsy increase the risk of local recurrence of invasive breast cancer? Breast J. 12:191-193, 2006.

10. Laeseke, P. F., T. C. Winter 3rd, C. L. Davis, K. R. Stevens, C. D. Johnson, F. J. Fronczak, J. G. Webster, and F. T. Lee Jr. Postbiopsy bleeding in a porcine model: reduction with radio-frequency ablation--preliminary results. Radiology 227:493-499, 2003.

11. Liu, Y. W., C. L. Chen, Y. S. Chen, C. C. Wang, S. H. Wang, and C. C. Lin. Needle tract implantation of hepatocellular carcinoma after fine needle biopsy. Dig. Dis. Sci. 52:228-231, 2007.

12. Moritz, A. R. and F. C. Henriques. Studies of Thermal Injury: II. The Relative Importance of Time and Surface Temperature in the Causation of Cutaneous Burns. Am. J. Pathol. 23:695-720, 1947.

13. Nilsson, E. and E. Fontes. Mathematical modelling of physicochemical reactions and transport processes occurring around a platinum cathode during the electrochemical treatment of tumours. Bioelectrochemistry 53:213-224, 2001.

14. Nilsson, E., H. von Euler, J. Berendson, A. Thorne, P. Wersall, I. Naslund, A. S. Lagerstedt, K. Narfstrom, and J. M. Olsson. Electrochemical treatment of tumours. Bioelectrochemistry 51:1-11, 2000.

15. Parker, B., S. Furman, and D. J. W. Escher. Input Signals to Pacemakers in a Hospital Environment. Ann. N. Y. Acad. Sci. 167:823-834, 1969.

16. Richards, R. N. and G. E. Meharg. Electrolysis: Observations from 13 years and 140,000 hours of experience. J. Am. Acad. Dermatol. 33:662-666, 1995.

17. Saulis, G., R. Lape, R. Praneviciute, and D. Mickevicius. Changes of the solution pH due to exposure by high-voltage electric pulses. Bioelectrochemistry 67:101-108, 2005.

18. Silva, M. A., B. Hegab, C. Hyde, B. Guo, J. A. Buckels, and D. F. Mirza. Needle track seeding following biopsy of liver lesions in the diagnosis of hepatocellular cancer: a systematic review and meta-analysis. Gut 57:1592-1596, 2008.

19. Stigliano, R., L. Marelli, D. Yu, N. Davies, D. Patch, and A. K. Burroughs. Seeding following percutaneous diagnostic and therapeutic approaches for hepatocellular carcinoma. What is the risk and the outcome? Seeding risk for percutaneous approach of HCC. Cancer Treat. Rev. 33:437-447, 2007.

20. Takamori, R., L. L. Wong, C. Dang, and L. Wong. Needle-tract implantation from hepatocellular cancer: is needle biopsy of the liver always necessary? Liver Transpl. 6:67-72, 2000.

21. Vijh, A. K. Electrochemical treatment (ECT) of cancerous tumours: necrosis involving hydrogen cavitation, chlorine bleaching, pH changes, electroosmosis. Int J Hydrogen Energy 29:663-665, 2004.

22. von Euler, H., E. Nilsson, J. M. Olsson, and A. S. Lagerstedt. Electrochemical treatment (EChT) effects in rat mammary and liver tissue. In vivo optimizing of a dose-planning model for EChT of tumours. Bioelectrochemistry 54:117-124, 2001.

23. Woitzik, J. and J. K. Krauss. Polyethylene sheath device to reduce tumor cell seeding along the needle tract in percutaneous biopsy. Surg. Endosc. 17:311-314, 2003.

24. Xin, Y., F. Xue, B. Ge, F. Zhao, B. Shi, and W. Zhang. Electrochemical treatment of lung cancer. Bioelectromagnetics 18:8-13, 1997.